Journal of Computational Electronics 2: 29–47, 2003

Simulating Ion Permeation Through the ompF Porin Ion Channel Using Three-Dimensional Drift-Diffusion Theory

T.A. VAN DER STRAATEN
Beckman Institute for Advanced Science and Technology, University of Illinois at Urbana-Champaign, 405 N Mathews Ave., Urbana, IL 61801, USA; Department of Molecular Biophysics and Physiology, Rush Medical College, 1750 W Harrison St., Chicago, IL 60612, USA

J.M. TANG
Department of Molecular Biophysics and Physiology, Rush Medical College, 1750 W Harrison St., Chicago, IL 60612, USA

U. RAVAIOLI
Beckman Institute for Advanced Science and Technology, University of Illinois at Urbana-Champaign, 405 N Mathews Ave., Urbana, IL 61801, USA

R.S. EISENBERG
Department of Molecular Biophysics and Physiology, Rush Medical College, 1750 W Harrison St., Chicago, IL 60612, USA

N.R. ALURU
Beckman Institute for Advanced Science and Technology, University of Illinois at Urbana-Champaign, 405 N Mathews Ave., Urbana, IL 61801, USA

Abstract. Ionic channels, natural nanotubes found in biological cells, are interesting to the electronics community because they display a range of device-like functions. The purpose of this paper is to illustrate how the solution methodology, developed for 3-D drift-diffusion models of semiconductor devices, can be applied to ion permeation in ionic channels. For this study we select the *ompF* porin channel, found in the membrane of the *E. coli* bacterium. The self-consistent 3-D model is based on the simultaneous solution of Poisson's equation, which captures Coulomb interactions, and a current continuity equation for each ion species, describing permeation down an electrochemical gradient. Water is treated as a uniform background medium with a specific dielectric constant. For demonstration, a simple model is assumed for the mobility/diffusivity of each ionic species and we compute the current-voltage relations for *ompF* porin in a wide range of conditions. Agreement with experimental measurements is surprisingly good given that the model uses the ion diffusivity as the only calibrated parameter.

Keywords: drift-diffusion simulation, numerical methods, ionic channels, bioelectronics, *ompF* porin

1. Introduction

Ion channels are a class of proteins found in the membranes of all biological cells. Each channel consists of a chain of amino acids folded in such a way that the protein forms a nanoscopic water-filled tunnel controlling ion transport through the otherwise impermeable membrane. An essential feature of proteins is that the

side chains of the amino acids (hereafter referred to as residues) are ionizable via the addition or subtraction of protons. The ionization state of a given residue depends on the pH and salt concentration of the solution in which the protein is immersed. Thus every ion channel carries a strong and steeply varying distribution of permanent charge, which depends on the particular combination of channel and prevalent physiological conditions. The charge distribution residing on the channel plays a critical role in determining the permeation characteristics of the open channel.

From a physiological standpoint ion channels regulate the transport of ions in and out of the cell, and in and out of compartments inside cells like mitochondria and nuclei, thereby maintaining the correct internal ion composition that is crucial to cell survival and function. Many channels have the ability to selectively transmit or block a particular ion species and most exhibit switching properties similar to electronic devices. Malfunctioning channels cause or are associated with many diseases, and a large number of drugs act directly or indirectly on channels (Ashcroft 1999). From a device point of view, ion channels can be thought of as elements in an electrical circuit, behaving like resistors, diodes or batteries depending on the specific channel and environmental factors. Some channels perform specialized functions resembling that of complex electronic systems. Indeed, equivalent circuit models have a long tradition in the theory of ion channels (Jack, Noble and Tsien 1975, Eisenberg, Barcilon and Mathias 1979).

The wide range of device-like functions exhibited by ionic channels has generated a great deal of interest in the engineering community. On the one hand, it is appealing to exploit the functionality of naturally occurring channels in traditional devices and circuits, e.g. for extreme miniaturization of sensors and achieve single molecule detection. On the other hand, a clear understanding of channel operation may provide a template for the design of functional elements based on synthetic molecular systems or nanotubes. The use of molecular elements for nanoscale integration would have the distinct advantage of perfect structure duplication and self-assembly, while the solid-state nanoscale device counterparts tend to be strongly affected by statistical fluctuations and defects. The methods of molecular genetics and biology often allow the control of channel proteins with atomic resolution. By replacing or deleting one or more of the amino acids many channels can be mutated, altering the charge distribution along the channel (http://hoshi-o.physiology.uiowa.edu/Mutations/Home.html). Engineering channels with specific conductances and selectivities is therefore conceivable. As device features continue to shrink the possibility, or perhaps, necessity of incorporating biological ion channels in the design of novel bio-devices becomes increasingly apparent.

With the availability of standardized software and computing power, Molecular Dynamics (MD) has become the most widely employed tool for studying ion dynamics in protein channels. Although MD simulations can resolve channel physics in atomic detail, the present computational requirements of such large-scale simulations prohibit the direct calculation of steady-state channel currents, particularly when channels are controlled by trace concentrations of ions or co-factors (Hille 2001). Alternatively, drift-diffusion theory, used widely in the engineering community (Selberherr 1984) to describe charge transport in semiconductor devices and plasma discharges, can be used to compute macroscopic current with a modest amount of computational effort. Drift-diffusion theory sacrifices the resolution of molecular detail. However, when used with an appropriate value of ion diffusivity it has been found to describe ion permeation through ion channels surprisingly well (Schuss, Nadler and Eisenberg 2001, Kurnikova *et al*. 1999, Hollerbach *et al*. 1999, Cardenas, Coalson and Kurnikova 2000, Eisenberg 1996, 1999).

In this paper we a present a self-consistent three-dimensional (3-D) drift-diffusion model of ion (K^+ and Cl^-) permeation through the *ompF* porin channel, a trimeric protein channel that spans the outer membrane of the *E. coli* bacterium to allow the passive diffusion of small hydrophilic solutes. *ompF* is one of the few channels whose three-dimensional molecular structure is well-known from X-ray crystallography (Tieleman and Berendsen 1998, Weiss and Schulz 1992, Schirmer 1998, Cowan *et al.* 1992, Philippsen *et al.* 2002). The porin molecule, shown in Fig. 1, is comprised of three identical intertwined polypeptide chains that form three separate identical pores through which ions can flow. Porin has an unusually stable arrangement that maintains its structural integrity well beyond the normal (eukaryotic) physiological range of salt concentrations, temperatures and applied voltages. About halfway along each pore the channel has a narrow constriction region, which is highly charged due to the presence of three positively charged (R42, R82, R132) and two negatively charged (D113, E117)

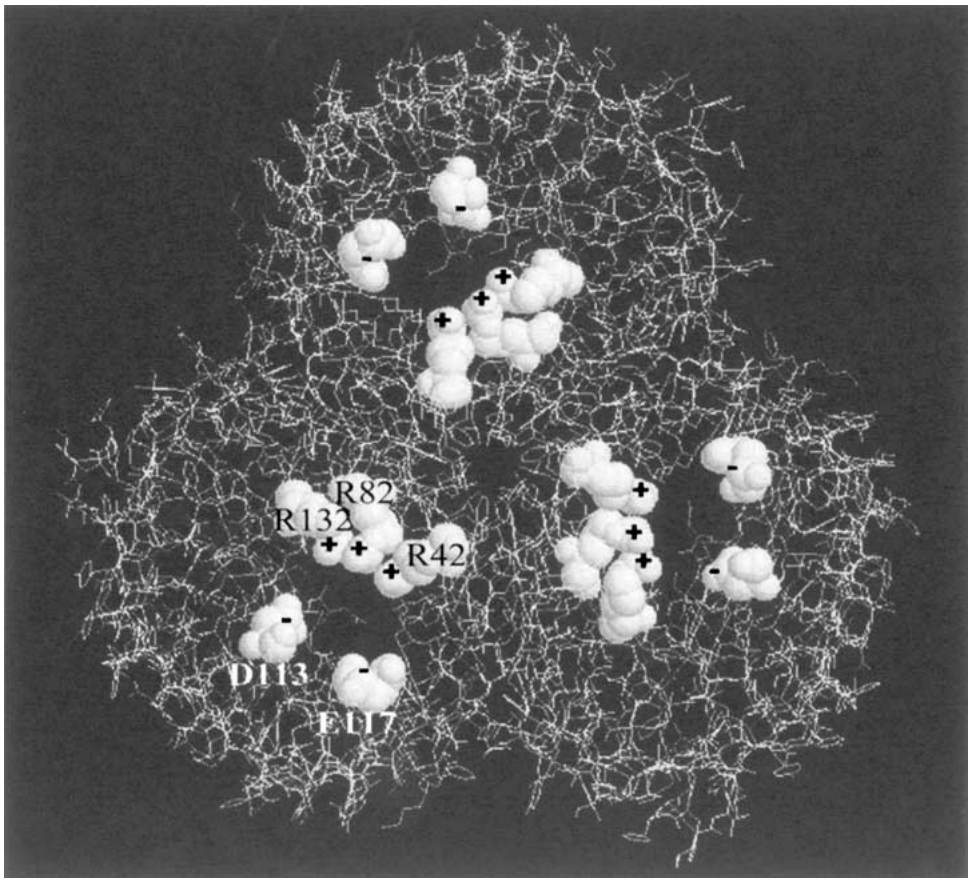

Figure 1. Molecular structure of *ompF*, a porin channel found in the outer membrane of the *E-coli* bacterium. This projection along the length of the channel shows the three-fold symmetry of the trimer. Several ionized residues in the constriction region of each pore are highlighted.

residues (Phale *et al.* 2001), as shown in Fig. 1. Here, R stands for *arginine* and E for *glutamate*, both acidic amino acid residues. The number identifies the location of the residue in the linear sequence of amino acids that form any protein. The arrangement of these charges gives rise to a very strong electric field transverse to the direction of ion flow, parallel to the plane of the membrane. The function of this transverse field is not known, although some of us believe it may be a binding site for a natural channel blocker, the identity of which is not yet known. Whatever the function, however, recent simulations (Im and Roux 2001, Schirmer and Phale 1999) show that it results in two separate strands of anionic and cationic current. The net charge residing on the entire porin molecule is equivalent to approximately $-30|e|$, where e is the electron charge.

The ease with which *ompF* can be mutated, together with its robust structure make *ompF* a good choice for experimental and computational studies and a possible template upon which to base the design of future biodevices. Here we use standard engineering Technology Computer Aided Design (TCAD) software to study ion transport in *ompF* porin over a wide range of conditions. In the following section we review drift-diffusion transport theory and discuss it's application to ion permeation through protein channels. A brief description of the TCAD software used to implement the model is also given, together with a discussion of the choice of physical parameters. In Section 3 we describe the experimental procedures followed in order to measure current-voltage curves for *ompF* porin. In Section 4 we compare those experimentally measured current-voltage curves with results computed from a self-consistent 3-D drift-diffusion model. The latter is also used to examine the channel selectivity (i.e., the preference for passing one ion species over another)

and average ion concentration in different regions of the channel. Section 5 summarizes the current work and outlines our plans to extend the drift-diffusion model to describe physical effects that are not adequately represented by the continuum theory in its present form.

2. Drift-Diffusion Transport Model

Drift-diffusion theory of charge transport is the cornerstone of classical transport theory. Although it is usual to compute the electric field self-consistently in most semiconductor device applications by coupling the transport equations with Poisson's Equation, in principle it is possible to use drift-diffusion theory with a given background field. Since the concept of evaluating the electrostatic potential self-consistently may be relatively unfamiliar to the ion channel community, we hereafter refer to drift-diffusion theory as Poisson Drift-Diffusion (PDD) theory, to avoid confusion and emphasize that the transport equations are coupled with Poisson's Equation. The theory is known as Poisson-Nernst-Planck (PNP) theory in the ion channel literature, where it was introduced independently but much later (Eisenberg 1996, Barcilon 1992, Barcilon, Chen and Eisenberg 1992, Barcilon *et al.* 1993). When fluxes are all identically zero, the theory is identical to (nonlinear) Poisson Boltzmann theory used to describe proteins (Eisenberg, Klosek and Schuss 1995, Antosiewicz *et al.* 1995, Sharp and Honig 1990, Honig and Nichols 1995, Warshel and Russell 1984). The drift-diffusion equation for the current density may be obtained from the lowest order moment of the Boltzmann equation (Ferry 1991), under the assumption that the distribution function is close to equilibrium. A consequence of this assumption is that in the diffusive term, obtained from moment integration of Boltzmann equation, one may use the average thermal energy for the carriers at the given temperature to evaluate the average of the square velocity, $\langle v^2 \rangle$, which can only be known if the distribution function is accessible. A discussion on the implications of assuming a near-equilibrium distribution function in the model hierarchy in semiconductor device simulation can be found in Ravaioli (1998). The drift-diffusion model is adequate not only in conditions of low bias voltage, but also when scattering events thermalize the carriers very quickly towards an equilibrium distribution, transferring to the environment the excess energy acquired by the carriers under the influence of the accelerating fields. Charged ionic carriers in a solution interact very strongly with water molecules. A model that treats ions as a plasma, moving in a continuum water background, can be described by the drift-diffusion set of equations presented later in this section, provided that the relaxation time for the charged ions in water is known, in order to define a mobility and a diffusivity (Chen *et al.* 1995). The tradition of device simulation, which spans half a century beginning with Shockley's seminal work on the semiconductor equations (Shockley 1950), has also shown that drift-diffusion theory can be extended successfully to carrier flow in conditions where mobility and diffusivity are space-dependent properties, as long as a local equilibrium is maintained by scattering, even if the device is subject to relatively large fields and current flow. The mathematical convenience of the drift-diffusion model has also motivated further empirical extensions where non-equilibrium conditions and heating of the carrier ensemble are established in the device (Selberherr 1984, Hess 2000, Lundstrom 1992). In such conditions, mobility and diffusivity become fitting parameters for the flow to match experimental current values, while the self-consistent density and potential distribution may be significantly deviating from the actual ones. This condition is not a concern for ionic currents in channels due to the high rate of thermalizing collisions with water. The use of a continuum conduction model raises instead some concerns when it is applied to flow in openings of restricted dimensionality. This may be the case in small ionic channels, when the actual diameter of the ion is comparable to the dimensions of the pore. Nonetheless, under these circumstances the continuum Poisson Drift-Diffusion model remains a useful tool to represent globally the input-output characteristics of the system, by formulating an equivalent flow with a fitted mobility in the constricted region, as long as one is aware that microscopic quantities like charge density may not be completely physical in the constricted region. In large measure Poisson Drift-Diffusion depends on conservation laws and simple constitutive equations. As long as these remain true in a certain domain of experimental and biological interest, the equations should be useful; indeed, they should capture the essence of what is happening, albeit perhaps with unphysical parameters. These limitations may be overcome, in part, by formulating corrections that take into account finite size of the carriers. It should clearly be noted that Poisson Drift-Diffusion automatically satisfies conservation and macroscopic constitutive laws, as does Monte Carlo simulations of

computational physics. On the other hand, molecular dynamics simulations in the tradition of protein chemistry do not, since they cannot predict current and therefore cannot satisfy Ohm's law or Fick's law (Eisenberg 1999), the latter invariably requiring thermostats to supply or remove kinetic energy every 10–100 femtoseconds.

2.1. *Theory*

The electrostatic potential ϕ is described by Poisson's Equation,

$$\nabla \cdot (\varepsilon \nabla \phi) = -(\rho_{\text{fixed}} + \rho_+ + \rho_-) \tag{1}$$

where ε is the dielectric constant and ρ_{fixed}, ρ_+ and ρ_- are the densities of fixed charge residing on the protein, and of mobile K^+ ions and Cl^- ions, respectively. The current density $j_\pm$ flowing down an electrochemical gradient is given by,

$$j_\pm = -(D_\pm / kT)\rho_\pm \nabla \psi_\pm \tag{2}$$

where $D_\pm$ is the diffusion coefficient and $\psi_\pm$ is the total electrochemical potential of each species, given by

$$\psi_\pm = q\phi \pm kT \ln \rho_\pm + \psi_\pm^{\text{ex}}$$

The first two components of $\psi_\pm$ describe the ideal chemical potential for a system of point charges. The last term $\psi_\pm^{\text{ex}}$, known as the "excess" chemical potential, accounts for departures from ideality due to the finite volume occupied by the ions (Davis 1996, Barthel, Krienke and Kunz 1998, Waisman and Lebowitz 1972a, 1972b, Durand-Vidal, Simonin and Turq 2000, Simonin and Blum 1996, Simonin, Bernard and Blum 1998, 1999, Simonin, Blum and Turq 1996, Simonin 1997, Nonner *et al.* 2001, Nonner, Catacuzzeno and Eisenberg 2000). Since most ion channels are typically only 4–8 Å wide while the permeating ions are 2–4 Å in diameter, the non-zero ion volume is likely to be important. Nonner, Gillespie and Eisenberg (2002) have recently combined a treatment of excess chemical potential using Density Functional Theory with one-dimensional drift-diffusion transport theory to describe ion permeation and selectivity for a calcium channel. Their results show that the finite volume of the ions is enough to account for most of the selectivity properties of channels, if they are computed at equilibrium with standard methods of modern physical chemistry. The work reported here was done at the same time as the work of Gillespie and Nonner and so finite volume effects will have to be considered in a later publication.

Upon setting $\psi_\pm^{\text{ex}} = 0$ the drift-diffusion Eq. (2) reduces to its more usual form

$$j_\pm = -(\mu_\pm \rho_\pm \nabla \phi \pm D_\pm \nabla \rho_\pm)$$

where the ion mobility $\mu_\pm$ is related to the diffusion coefficient via the Einstein relations. Conservation of charge is enforced via the continuity equation

$$\nabla \cdot j_\pm + \frac{\partial \rho_\pm}{\partial t} = S_\pm \tag{3}$$

where $S_\pm$ captures the details of ion binding and other chemical phenomena that may populate or deplete the ion densities. We do not consider such phenomena in this present work and set $S_\pm = 0$.

The channel system contains a single porin molecule *in situ* in a lipid bilayer (membrane), immersed in an aqueous bath of KCl. The three pores provide an aqueous pathway for K^+ and Cl^- ions to cross the bilayer. Experimentally different salt concentrations are set on either side of the bilayer (hereafter referred to as C_{left} and C_{right}). Electrodes are immersed in the baths to maintain a fixed bias voltage across the channel/membrane system. We seek a steady-state solution for ϕ, ρ_+ and ρ_- that simultaneously satisfies the coupled partial differential equations (PDEs) (1)–(3) subject to the following Dirichlet boundary conditions (4) enforced at the electrodes.

$$\begin{aligned} \phi^{\text{right}} - \phi^{\text{left}} &= V_{\text{bias}} \\ \rho_{\pm,\text{right}} &= C_{\text{right}} \\ \rho_{\pm,\text{left}} &= C_{\text{left}} \end{aligned} \tag{4}$$

2.2. *The PROPHET Simulator*

Equations (1)–(4) are a set of highly nonlinear, coupled PDEs, and are notoriously difficult to solve numerically, even for relatively simple systems. Due to their extensive application in the transport theory of semiconductor devices much attention has been paid to developing robust and stable numerical schemes for solving these equations in time and three-dimensional space (Selberherr 1984, Bank, Rose and Fichtner 1983, Bank *et al.* 1990). Well-tested packages for discretizing and solving the Eqs. (1)–(4) on two-dimensional

(2D) and three-dimensional (3-D) meshes in feasible runtimes on workstations are now readily available (http://www.ise.ch, http://www.synopsys.com, http://www.silvaco.com). However, most of these solvers are oriented toward the simulation of semiconductor devices for which the system geometry is relatively simple. Application of "off-the-shelf" packages to geometrically complex systems such as those found in ion channels is generally not possible since the latter requires a detailed representation of the channel geometry.

The model described above was implemented using the PROPHET simulator (http://www-tcad.stanford.edu/∼prophet/), a computational platform originally developed at Lucent Technologies for semiconductor process modeling, and currently being extended to include a variety of device simulation models at Stanford University. The PROPHET simulator provides a convenient scripting framework for defining, discretizing and solving an arbitrary system of PDEs. Physical properties such as dielectric constant and mobility can be assigned to the different regions of the computational domain at run-time.

Equations (1)–(4) are readily constructed using existing PROPHET operators, and discretized using finite volume methods. The resulting system of nonlinear algebraic equations is then solved by Newton's method, using sparse iterative techniques (Selberherr 1984). In contrast to most commercial PDE solvers, PROPHET has the flexibility of being able to handle arbitrary geometries such as those encountered in biological systems. A customized mesh, shown in Fig. 2, was created for the *ompF* molecular structure, defining three regions—protein, membrane and electrolyte—on a 1.5 Å uniform rectilinear mesh. The protein and membrane are assigned relative dielectric constants of 20 and 2 respectively, and the electrolyte is assigned a value of 80. There are two electrodes placed at opposite ends of the domain approximately 15 Å from the ends of the porin molecule as shown.

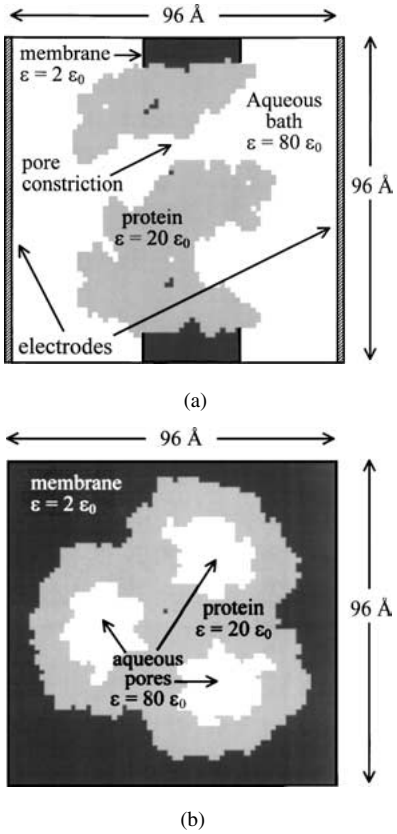

Figure 2. PROPHET mesh representation of the *ompF* trimer *in situ* in a membrane, immersed in an electrolyte solution (potassium chloride) showing (a) longitudinal and (b) cross-sectional slices through the 3-D computational domain generated on a uniform rectilinear grid (1.5 Å mesh size). Electrodes placed at both ends of the domain maintain a fixed bias across the channel/membrane system.

2.3. *Physical Parameters*

The density of fixed charge on the protein, ρ_{fixed} was modeled by associating a fractional point charge (in units of $|e|$) to each atom, and then interpolating the charge to the mesh. The charges residing on isolated amino acids in neutral electrolyte solutions can be calculated using *ab initio* quantum chemistry codes. Here we have used the tabulated OPLS partial charges, a force field used widely in MD simulations of protein molecules (Jorgensen 1998, Jorgensen and Tirado-Rives 1988), with modifications to account for the dielectric environment, proximity of neighboring amino acids in the folded of the protein, and electrolyte concentration (van der Straaten *et al.* 2002, Antosiewicz, McCammon and Gilson 1994).

The diffusion coefficient for ions freely diffusing in bulk electrolyte transport can be inferred from experiments (Tyrrell and Harris 1984, Newman 1991, Harned and Owen 1958, Robinson and Stokes 1959, Conway 1969, Zematis *et al.* 1986) and is well documented in the literature (Barthel, Krienke and Kunz 1998, Durand-Vidal, Simonin and Turq 2000, Newman 1991, Robinson and Stokes 1959, Conway 1969, Zematis *et al.* 1986, Conway, Bockris and Yaeger 1983, Schmickler 1996, Berry, Rice and Ross 2000, Barthel,

Buchner and Münsterer 1995). In the confined volumes of ionic channels, where additional sources of friction (Kurnikova, Waldeck and Coalson 1996, Nee and Zwanzig 1970, Wolynes 1980, Bagchi and Biswas 1998) will also restrict ion motion, the diffusion coefficient is expected to differ from bulk values, and cannot be obtained by experimental means. Recent MD simulations of K^+ and Cl^- ions inside the porin channel indicate that the diffusion coefficient is substantially reduced from its bulk (van der Straaten *et al.* 2002). However, physical analysis of the diffusion coefficient, even in homogeneous ionic solutions, presents major difficulties for MD (Evans and Morriss 1990, Ciccotti and Hoover 1990, Hoover 1986, 1991, Alder 1992, Mareschal and Holian 1992). In the inhomogeneous environment of an ion channel, where ion transport is governed by atomic motions occurring over extremely disparate time-scales, the determination of the diffusion coefficient from MD poses considerable difficulties in principle as well as practice: it is possible that estimating an effective diffusion coefficient requires a simulation in atomic detail *on the time scale of experimental measurements* (i.e., milliseconds). Such simulations are not likely to become practical in the near future, particularly if they depend in an important way on the trace concentrations of ions.

For this reason we have adopted an engineering approach, assuming a spatially uniform diffusion coefficient. Since we compute the current-voltage relations for potassium chloride KCl, for which the diffusion coefficients in bulk electrolyte are approximately the same for both species ($D_{K+} = 2.00 \times 10^{-5}$ cm^2 s^{-1}, $D_{Cl-} = 1.98 \times 10^{-5}$ cm^2 s^{-1} (Lide 1994)), we assume the same constant diffusion coefficient for each ion species $D_+ = D_- = D$. In that case the computed current scales linearly with the diffusion coefficient (Eq. (2)), and can be adjusted to give the best fit to the measured curves, yielding an appropriate value for the effective diffusion coefficient. The simulations presented here with the choice of diffusivities illustrated above should be taken mainly as demonstration of the TCAD approach with PROPHET. The use of a best fit for the diffusivities follows a purely engineering approach. From a physical point of view, each ionic species may be characterized by its own diffusivity that is spatially dependent inside the channel. The simple choice of uniform diffusivity fit followed in this paper does not affect the generality and robustness of the solution approach. Work is in progress to determine space-dependent diffusivities for the porin channel using Molecular Dynamics simulations, and we plan to report on these results later.

3. Experiments

In this section we describe the experimental protocols followed in order to record single-channel current-voltage curves for *ompF* porin, which were used to calibrate the value of the effective diffusion coefficient. The importance of using a single porin molecule for these measurements cannot be overstated: measurements from an ensemble of channels are difficult to interpret because they include channels that insert with opposite orientations. The measured properties depend on the orientation (because the molecule is asymmetrical) and the orientation of insertion is not the same under different experimental conditions (because the charge density on the protein which helps control insertion is asymmetrical and varies with experimental conditions). Thus, measurements must be made on single trimers if they are to be reliable.

3.1. Porin

The porin protein *ompF* was provided in a solution containing 100 mM KCl, 1 mM *EDTA*, 20 mM NaH_2PO_4 and 1% detergent *n*-octyl-polyoxyethylene (O-POE: product number P-1140, Bachem Bioscience Inc., King of Prussia, PA 19406) and then diluted into a 100 mM KCl solution containing 1% O-POE. Solutions were buffered with 20 mM HEPES (pKa = 7.55) to pH 7.4. Porin molecules were reconstituted one at a time into a painted planar bilayer stretched over a 150 μm aperture, area $\sim$0.02 mm^2, separating 4 ml of salt solution in a grounded bilayer chamber and 3 ml of salt solution in a Delrin cup. Ag/AgCl electrodes were connected to the bathing solution by 3 M KCl-3% agar bridges to minimize liquid junction potentials. To minimize electrical and mechanical artifact, solutions were stirred with a dc powered magnetic stirrer (Cole Palmer, Model 4804, using a micro-stirring bar) and changed in the grounded bilayer chamber (held at zero potential) using two peristaltic pumps with constant flow.

3.2. Bilayers

Bilayers were made from lipids *phosphatidylethanolamine* (#840022 from Avanti Polar Lipids,

Alabaster, AL 35007) and *phosphatidyl-choline* (#840053) dissolved in chloroform. Lipids (PE:PC 4:1) were evaporated with argon, dissolved in *n*-Decane (Sigma D4384) at a concentration of 10 mg/ml and used within 2 weeks. Otherwise, insertion was rarely observed. The resistance from the ground chamber to the voltage bath chamber was ∼50–100 GΩ. Experiments were started with 0.1 M, 0.25 M, or 0.5 M KCl salt solutions on both sides of the bilayer. Porin (0.1 ng) was then placed in the 4 ml of the grounded chamber and insertion of a single trimer was typically observed after 5–10 minutes of stirring. The solution on the grounded side was changed after a trimer inserted. Single channel currents were recorded from the same porin trimer with a range (0.1 M to 3 M KCl) of solutions on the grounded side.

3.3. Current Measurements

With these precautions, it was possible to measure single channel currents in the same porin trimer in many solutions: recordings were made from the *same* porin trimer with 0.1, 0.25, 0.5, 1, and 3 M KCl solutions on the grounded side. The solution in the voltage chamber was not changed when recording from one porin trimer, although, of course, that solution was different in different experiments, i.e., 0.1, 0.25 and 0.5 M. Current was recorded in response to step or ramp potentials, with current-voltage characteristics being measured with ramps. The gating processes that open and close porin were not studied. Figure 3 shows a typical histogram of the currents through a single porin molecule with 1 M solutions of KCl on either side of the bilayer under an applied voltage of −100 mV. Current peaks occurring at regular intervals indicate the number of conducting pores, the largest current corresponding to all three pores being in the open state, for example. Figure 4 shows the traces of current as a function of time after bias voltages of (a) +80 mV and (b) −80 mV are applied. The four evenly spaces levels of current correspond to all three pores closed (zero current), and one, two or all three pores open.

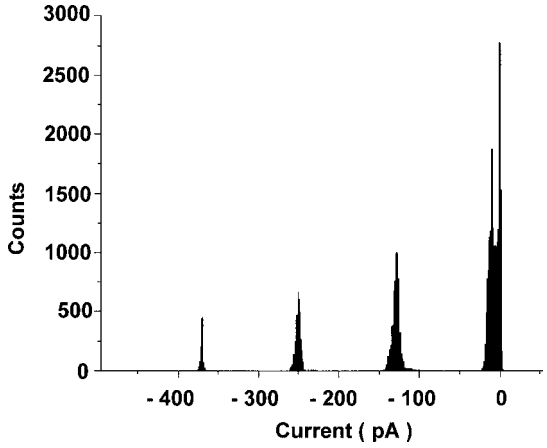

Figure 3. The amplitude histogram of the currents through a single trimer of *ompF* reconstituted into a lipid bilayer, in a symmetric 1 M KCl solution under −100 mV applied voltage. The four main peaks at 0 ± 2.5 pA (Baseline), 128 ± 3.7 pA, 250 ± 2.4 pA and 370 ± 1.0 pA correspond to current flowing through none, one, two and three pores. In addition the graph exhibits a smaller peak at 10 ± 3.8 pA (pedestal current), the origin of which is not yet known. The conductances of the individual pores are similar at about 1.2 nS while the conductance of the pedestal current is about 10 times smaller. The seal resistance was 20 GΩ.

4. Simulations

4.1. Nernst Potential

The net flux of particles in a system that has reached thermodynamic equilibrium is zero. Simulations of ion channels and proteins are almost always done at equilibrium (Tieleman and Berendsen 1998, Roux and Karplus 1991a, 1991b, Roux 1999, Tieleman *et al.* 2001). However, the primary function of ion channels—the translocation of ions—takes place only when the system is driven away from equilibrium. An electrochemical gradient must be present to cause a net flow of ions through the channel. The Nernst Potential is the holding potential required to balance a density gradient across a barrier having an aperture that allows only one species of ion to flow, such that the net flow of charge is zero (Newman 1991)

$$V_{\text{Nernst}} = -\frac{kT}{q} \ln\left(\frac{C_{\text{left}}}{C_{\text{right}}}\right) \tag{5}$$

where C_{left} and C_{right} are the concentrations of the permeable ion on either side of the barrier. The PROPHET package has been extensively used in process and device simulation, and its accuracy has been proven by solving a range of problems in the semiconductor area. We nonetheless verify the accuracy of PROPHET by computing the Nernst Potential for a simple three-dimensional barrier structure, shown in Fig. 5. The fixed charge ρ_{fixed} was set to zero and Eqs. (1)–(4) were solved for a range of concentration gradients

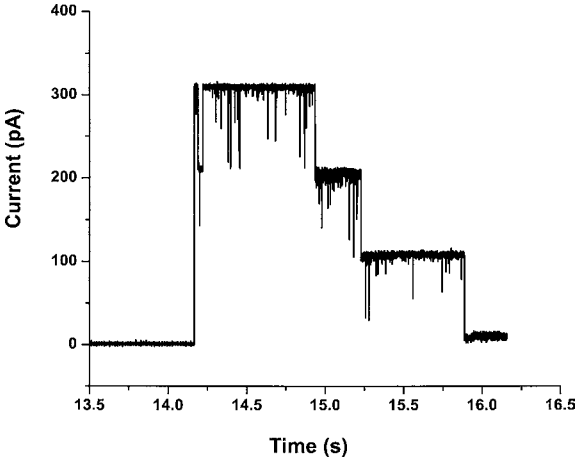

(a)

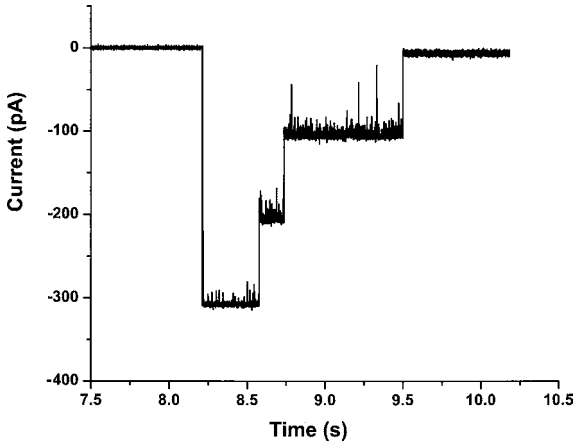

(b)

Figure 4. Current through a single trimer of *ompF* as a function of time under bias voltages of (a) +80 mV and (b) −80 mV. In addition to the four main conductance states (none, one, two and three pores) these current traces show evidence of many short-lived subconductance states.

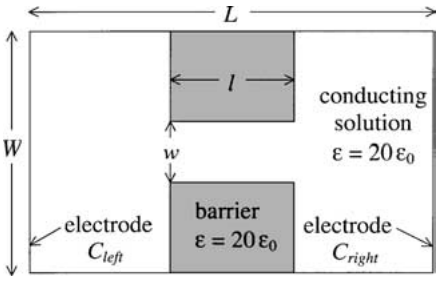

Figure 5. Barrier structure used to compute the Nernst potential. The width W, depth W and length L of the three-dimensional simulation box were all set to 96 Å.

Table 1. Nernst potential for a barrier structure.

l/L	w/W	$C_{\text{right}}/C_{\text{left}}$	V_{Nernst} (mV) (Eq. (5))	V_{Nernst} (mV) (PROPHET)
1/2	1/4	2.5	−23.7	−23.7
		5	−41.6	−41.6
		10	−59.5	−59.3
1/2	1/8	2.5	−23.7	−23.8
		5	−41.6	−41.7
		10	−59.5	−59.1
1/4	1/8	2.5	−23.7	−23.7
		5	−41.6	−41.6
		10	−59.5	−59.2

($C_{\text{left}}/C_{\text{right}}$), applied biases, barrier thickness l and square aperture widths w. The KCl concentration on the left side of the barrier was held fixed at $C_{\text{left}} = 0.1$ M KCl while the concentration on the right side was varied between 0.25 and 1 M. K^+ was chosen to be the permeable ion by suppressing the Cl^- diffusivity by a factor of 10^3 relative to the K^+ diffusivity. For all combinations of conditions the PROPHET simulator matches the theoretical value of the Nernst Potential given by Eq. (5) to within 0.5%. Table 1 summarizes the results.

4.2. *Current-Voltage Relations*

After verifying the Nernst potential, PROPHET was used to solve the coupled system (1)–(4) in the porin channel for various salt concentrations and applied biases corresponding to experimental measurements described in Section 3. To provide suitable initial conditions, PROPHET was used to first solve the nonlinear Poisson equation (referred to as the Poisson-Boltzmann Equation in ion channel literature) under conditions of zero concentration gradient (symmetric bath concentrations $C_{\text{left}} = C_{\text{right}}$). The standard continuation method is adopted, where the current-voltage (I-V) curves are built by generating a sequence of solutions with slightly increased bias each time, with the previous solution as initial condition. The method of continuation was applied to obtain the steady-state ion densities and potential profiles for asymmetric solutions ($C_{\text{left}} \neq C_{\text{right}}$) under zero applied bias. Using the zero-bias solutions as an initial condition the full system (1)–(4) was solved for each set of bath concentrations, using continuation in the applied potential over a range values of physiological interest (±200 mV).

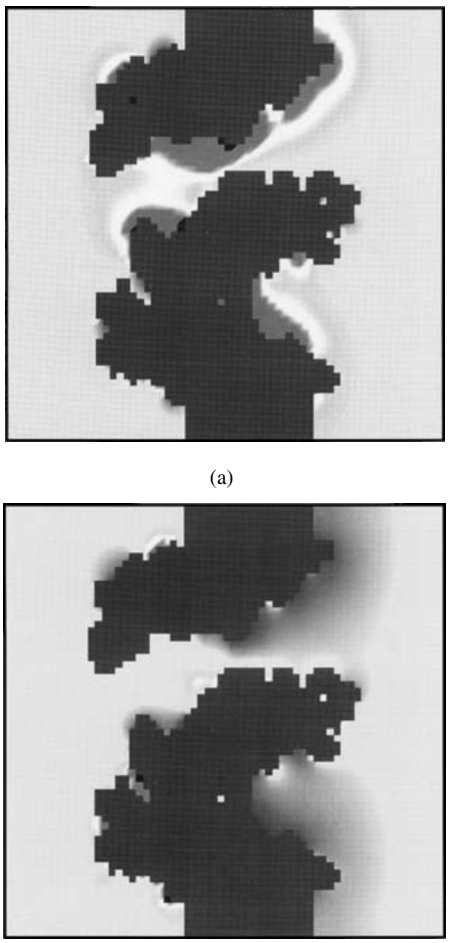

Figure 6. Steady state (a) K^+ ion density and (b) Cl^+ ion density on a two-dimensional slice through the computational domain for a 0.1 M symmetric ($C_{\text{left}} = C_{\text{right}}$) KCl under an applied bias of 200 mV.

Typical performance on the NCSA SGI Origin 2000 allows 15 current-voltage curves to be calculated in approximately 36 CPU hours.

Figure 6 shows the steady state ion densities, (a) K^+ ion density and (b) Cl^- ion density, on a 2D slice intersecting one of the three pores. A bias voltage $V_{\text{bias}} = 200$ mV was applied across the electrodes. The concentration of KCl electrolyte in the baths on either side of the membrane was held at $C_{\text{left}} = C_{\text{right}} = 0.1$ M ($1\text{ M} = 1000 N_A\text{ m}^{-3}$, where $N_A = 6.02 \times 10^{26}$ is Avogadro's number). As expected, ions accumulate in regions of strong fixed charge residing on the amino acids.

Figure 7 compares the experimentally measured I-V curves obtained in symmetric solutions of (a) 0.1 M, (b) 0.25 M, (c) 0.5 M and (d) 1 M KCl with those computed from the drift-diffusion model. At lower salt concentrations (0.1 M and 0.25 M) the measured I-V curves, shown by the unbroken line, exhibit a significant departure from linearity and an asymmetry with respect to the applied bias. This weakly rectifying behavior is also evident from the simulation results (shown by symbols), and reflects the longitudinal asymmetry inherent in the distribution of fixed charges lining the channel. The agreement between experiment and simulation is reasonable, considering that the latter were computed with spatially uniform diffusion coefficients. As the salt concentration is increased, the non-linearity disappears suggesting more effective electrostatic shielding of the charges lining the pore of the channel. At higher salt concentrations (0.5 M and 1 M KCl), the computed I-V curves fit the experiment very well.

Separate fits were performed for each set of concentrations shown in Fig. 7, giving effective diffusion coefficients in the range $D = (0.58\text{–}0.67) \times 10^{-5}\text{ cm}^2\text{ s}^{-1}$. These values are comparable to the average diffusion coefficient inside the channel obtained from Molecular Dynamics simulations (van der Straaten *et al.* 2002). Unlike the free diffusion of ions in bulk electrolyte solution, ionic transport inside the restricted and highly charged volume of an ion channel is likely to be a dynamic coupled function of the protein and its environment. As such it is hardly surprising that the effective diffusion coefficient varies with salt concentration. In fact, Schirmer and Phale (1999) have shown that the pathways for diffusion of anions and cations in *ompF* are separate. It would be remarkable if this bifurcation in pathways did not result in a concentration dependent diffusion coefficient. For comparison, the same fitting procedure was applied to the entire data set covering all four concentrations, yielding a single effective diffusion coefficient $D = 0.63 \times 10^{-5}\text{ cm}^2\text{ s}^{-1}$. Again, the agreement between the experimental and computed I-V curves, shown in Fig. 8, is reasonable.

The role of the fixed charge lining the pore of the channel in determining the channel's I-V characteristic is clearly demonstrated in Fig. 9, which compares the I-V curves for symmetric solutions of 0.1 M KCl computed with (solid lines, filled symbols) and without (dashed lines, open symbols) the fixed charge. The individual cationic and anionic, and the net current is shown for each case. There are three specific observations to be made from Fig. 9. Firstly, in the absence of permanent fixed charge on the protein, the I-V curve exhibits a bowing and the total current is symmetric

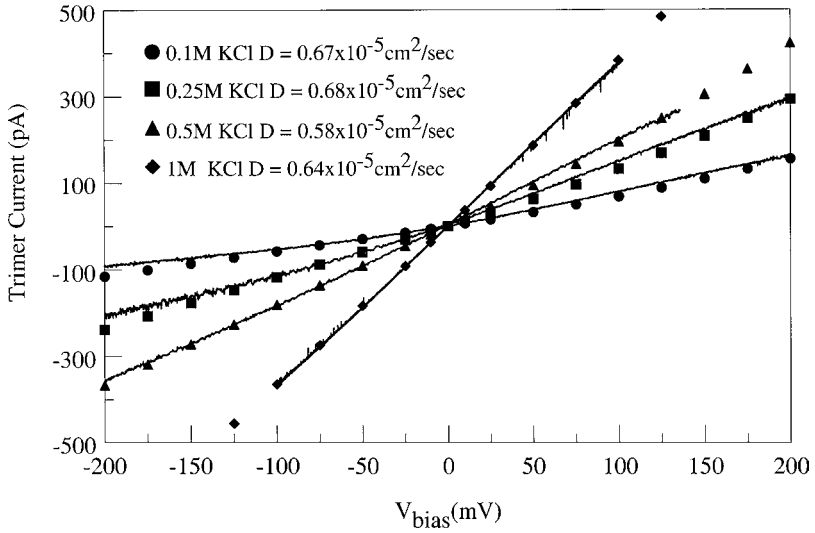

Figure 7. I-V curves computed for symmetric solutions of (a) 0.1 M (●$D = 0.67 \times 10^{-5}$ cm^2 s^{-1}), (b) 0.25 M (■ $D = 0.68 \times 10^{-5}$ cm^2 s^{-1}), (c) 0.5 M (▲ $D = 0.58 \times 10^{-5}$ cm^2 s^{-1}) and (d) 1 M (♦$D = 0.64 \times 10^{-5}$ cm^2 s^{-1}) KCl. Experimentally measured curves, indicated by the continuous line, are shown for comparison. The diffusion coefficient that provides the best fit to the measured I-V curve was determined separately for each concentration.

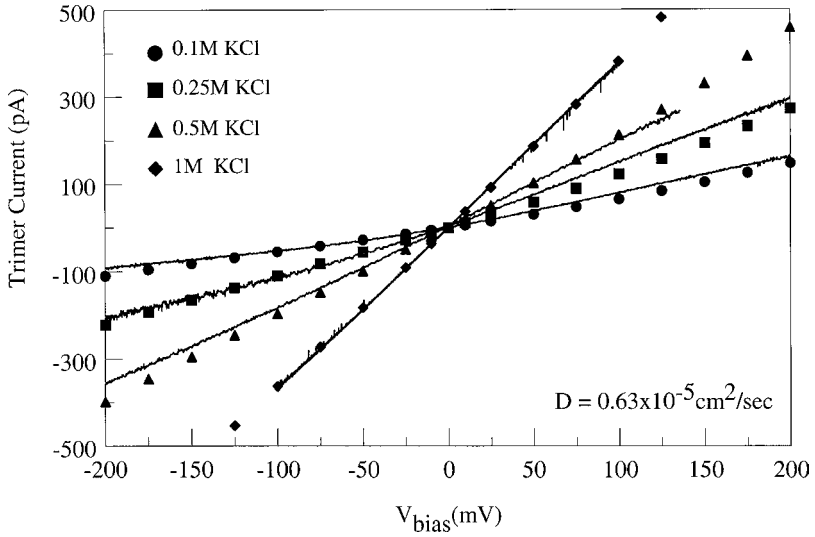

Figure 8. Measured and computed I-V curves in symmetric solutions (a) 0.1 M (●), (b) 0.25 M (■), (c) 0.5 M (▲) and (d) 1 M (♦) KCl. The symbols represent the I-V curves computed using a single value of diffusion coefficient ($D = 0.63 \times 10^{-5}$ cm^2 s^{-1}) that gives the best fit to the entire set of measured data.

with respect to the magnitude of the applied bias. Secondly, in the absence of fixed charge the model predicts a slight selectivity that depends on the polarity of the applied bias. For positive bias the channel favors cationic current, while for negative bias it favors anionic current. The individual cation and anion I-V curves are slightly rectifying but add to yield a total current that is still symmetric. This behavior, which is contrary to what is observed for a simple aperture, suggests that the highly irregular channel geometry favors ion flow in a specific direction. With reference to Fig. 6 this preferential flow is from the right electrode, held at ground potential, to the left electrode where the bias is applied. Lastly, when the non-uniform permanent

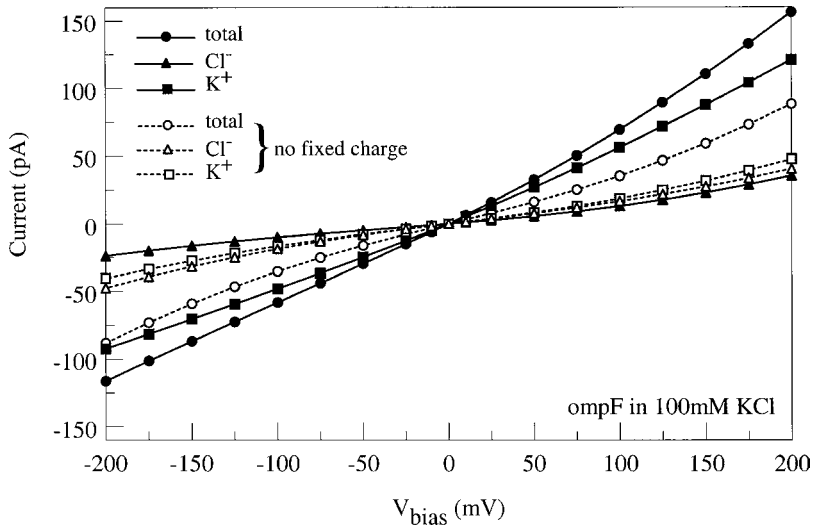

Figure 9. Computed I-V curves for symmetric solutions of 0.1 M KCl computed with (solid lines, filled symbols) and without (dashed lines, open symbols) the fixed charge. The individual K^+ (■) and Cl^- (▲), and the net current (●) is shown for each case.

fixed charge of approximately $-30|e|$, is included in the model the channel now becomes significantly selective for cation current irrespective of the bias polarity. The combination of the geometry-induced selectivity and that induced by the fixed charged would explain to some extent the mild rectifying behavior in the complete I-V curve. We conclude that it is important to use a realistic three-dimensional channel geometry to capture the details of the transport in ionic channels.

It is very important to study asymmetric solutions because the I-V curves predicted by traditional barrier and diffusion models, which do not compute the local electric field in a self-consistent manner, are strikingly different from those predicted by models that compute the electric field consistently (Hille 2001, Eisenberg 1996, 1999, Chen and Eisenberg 1993). Figure 10(a)–(c) compare the experimental I-V curves measured in asymmetric concentrations of KCl with those computed from the drift-diffusion model. The discontinuities evident in some of the experimental data indicate that the channel has closed spontaneously over that particular range of applied voltages. Each figure corresponds to experimental conditions in which the concentration of KCl in one bath, C_{left}, is held constant while the concentration in the other, C_{right}, is varied. For each value of C_{left} the spread in effective diffusion coefficients is fairly small (within 4 to 8% of the average). Interestingly, the value of diffusion coefficient that provides the best fit to the measured curve is not the same when the bath concentrations are swapped. That is, the effective diffusion coefficient depends on the alignment of the porin molecule with respect to the baths, e.g., for $C_{\text{left}} : C_{\text{right}} = 100$ mM : 250 mM we find $D = 0.64 \times 10^{-5}$ cm^2 s^{-1} while for $C_{\text{left}} : C_{\text{right}} =$ 250 mM : 100 mM we find $D = 0.74 \times 10^{-5}$ cm^2 s^{-1}. This result is hardly surprising considering the evident asymmetry of the molecule but it has the unfortunate effect of making measurements of properties of ensembles of channels difficult to interpret.

4.3. Channel Selectivity

Porin is known to be moderately selective for cations (over anions) (Schirmer 1998, Im and Roux 2001, Saint *et al.* 1996a, 1996b, Schindler and Rosenbusch 1978, Mauro, Blake and Labarca 1988, Young *et al.* 1983). This preference for cations may be attributed in most part to the overall negative charge residing on the protein. Here we use the fraction of total current carried by K^+ ions, computed with the drift-diffusion model, as a measure of the channel selectivity for cations over anions—alternative measures of channel selectivity are discussed in Gillespie and Eisenberg (2002). Figure 11 shows the fractional K^+ current as a function of salt concentration at a fixed applied bias of 100 mV. At high salt concentrations, where Coulombic shielding of the fixed charge is likely to be stronger (Schirmer 1998, Im and Roux 2001, Saint *et al.* 1996a, 1996b, Schindler and Rosenbusch 1978), simulations predict a very weak

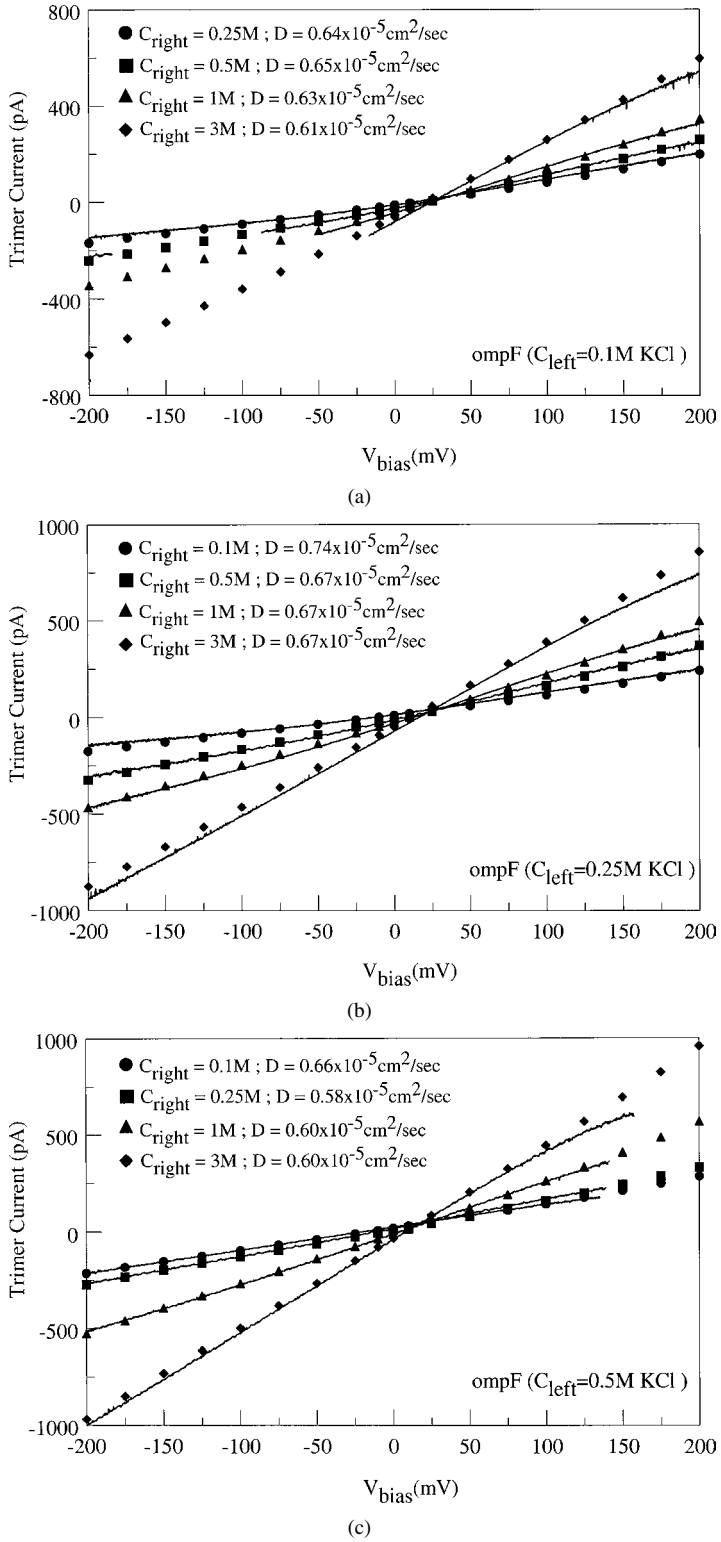

Figure 10. Experimentally measured and computed I-V curves obtained in asymmetric solutions of KCl, for salt concentrations in the left bath of (a) 100 mM, (b) 250 mM and (c) 500 mM.

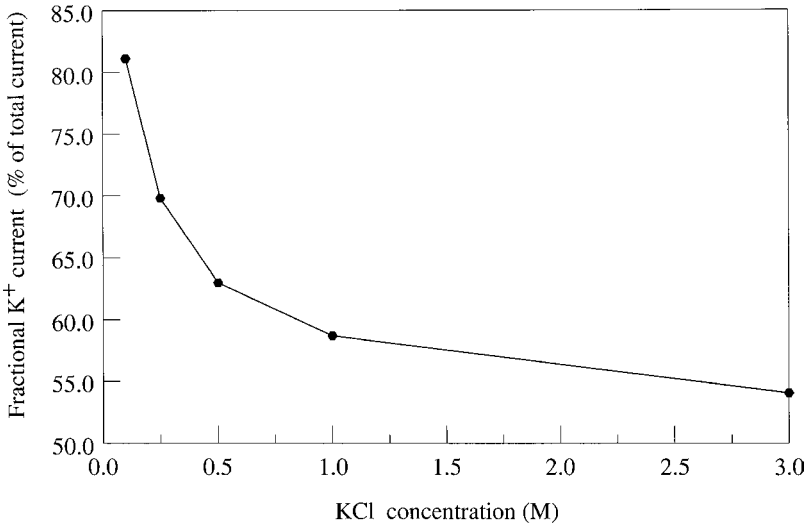

Figure 11. K^+ selectivity, defined here as the fraction of total current carried by K^+ ions, as function of KCl concentration, at a fixed applied voltage of 100 mV.

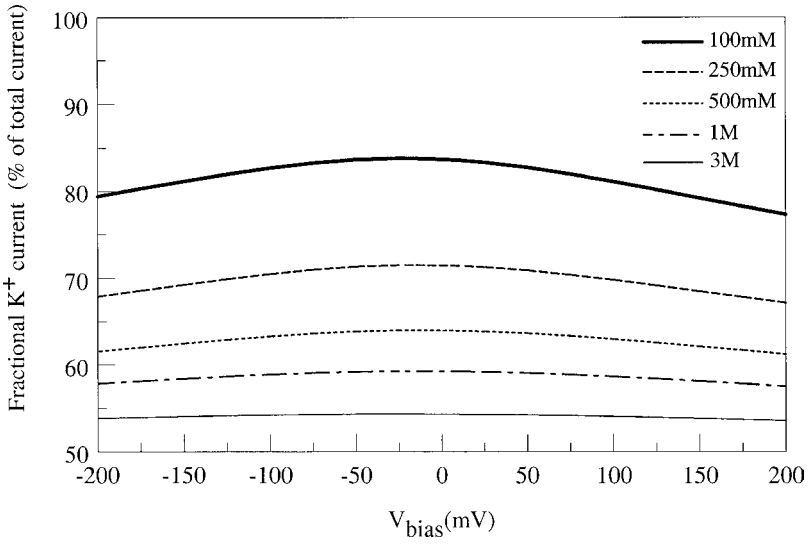

Figure 12. K^+selectivity as a function of applied voltage, for various of symmetric concentrations of KCl.

preference for cationic current, with roughly 54% of the current being carried by K^+ ions in 3 M KCl. As the salt concentration is reduced, the channel becomes increasingly selective for cationic current, with more than 80% of the total current being carried by K^+ ions at 0.1 M KCl. However, when simulations are conducted again with the fixed charge removed to test its effect, the fractional K^+ current in 0.1 M KCl drops to about 50%, confirming that the channel selectivity is strongly linked to the degree to which the fixed charges on the protein are screened by the mobile charge inside the pore. Electrostatic screening effects alone do not determine channel selectivity. There are issues related to the finite ion size that have been shown to dominate the selectivity in some channels. Volume exclusion effects are not addressed in the present model, which treats the ions as a charged fluid.

Figure 12 shows the computed fractional K^+ current as a function of applied voltage, for various symmetric bath concentrations. At low salt concentrations (0.1 M)

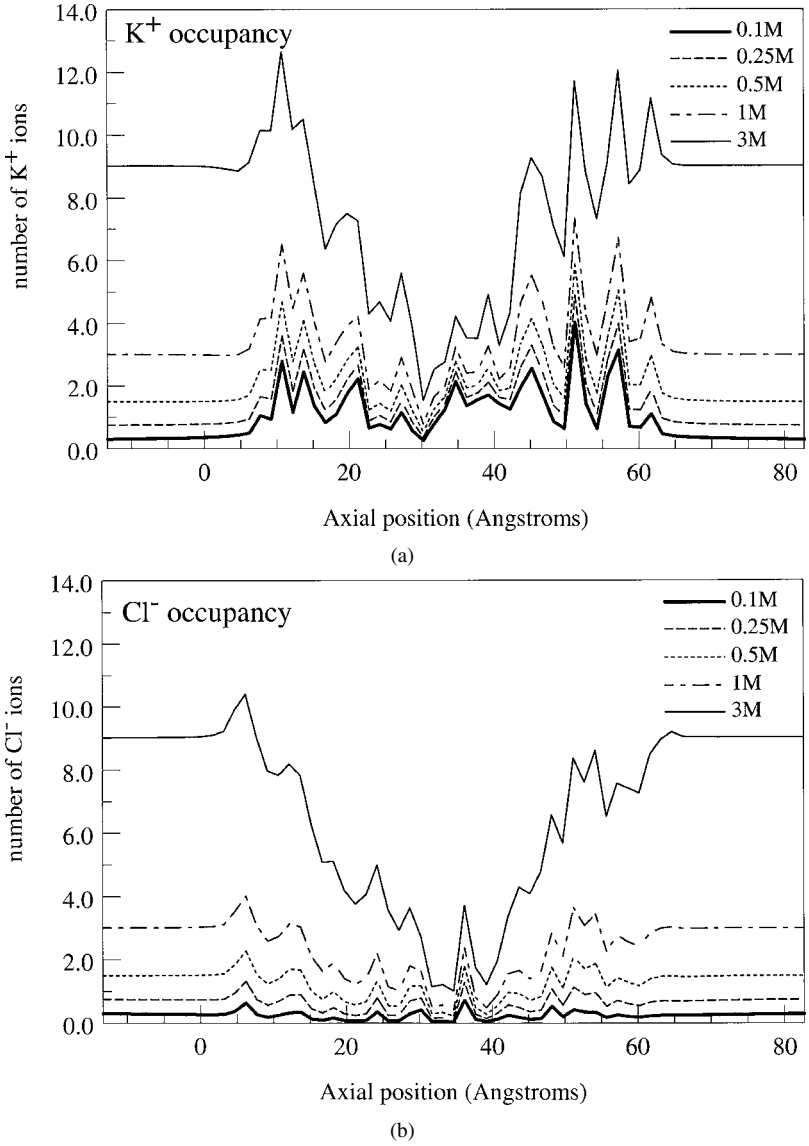

Figure 13. Equilibrium (no applied voltage) ion occupancy as a function of axial position along the pore for (a) K^+ and (b) Cl^- for symmetric bath concentrations of 0.1 M, 0.25 M, 0.5 M, 1 M and 3 M KCl.

the fractional K^+ current is weakly dependent on applied voltage, decreasing slightly as the magnitude of the applied bias increases. As the bath concentration is increased, the fraction of current carried by K^+ ions decreases and the mild dependence on applied bias disappears altogether.

4.4. Ion Occupancy

The ion occupancy—the integral of the ion concentration—in a given region of the channel represents the average number of ions likely to be found there at any given time. Figure 13 shows (a) K^+ and (b) Cl^- ion occupancy profiles in the direction normal to the lipid membrane and electrodes, under conditions of zero bias, for the same five symmetric KCl bath concentrations. The occupancy exhibits a similar profile at all concentrations. Near the mouths of the channel, the K^+, and to a lesser extent, the Cl^- occupancies increase from their values in the bulk solution. Inside the channel the K^+ occupancy is greater than in the bulk electrolyte surrounding

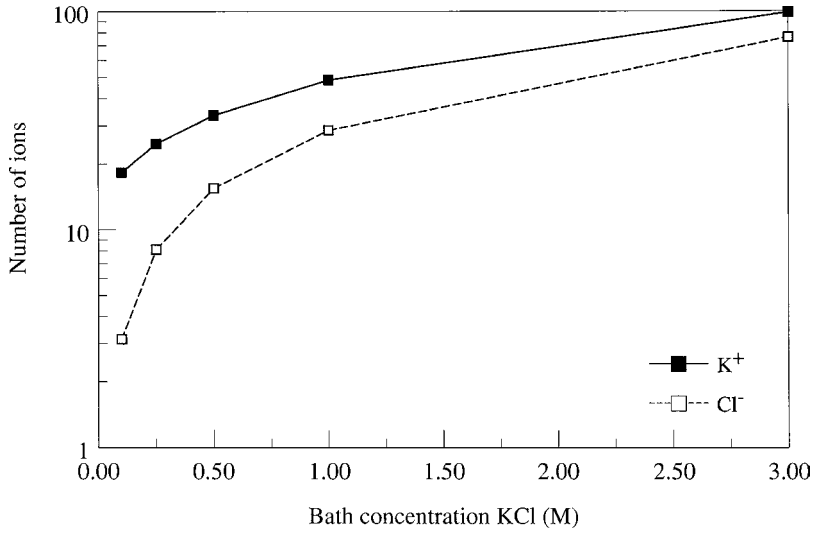

Figure 14. Net K^+ and Cl^- occupancies for a single pore of the *ompF* trimer as a function of symmetric KCl bath concentration.

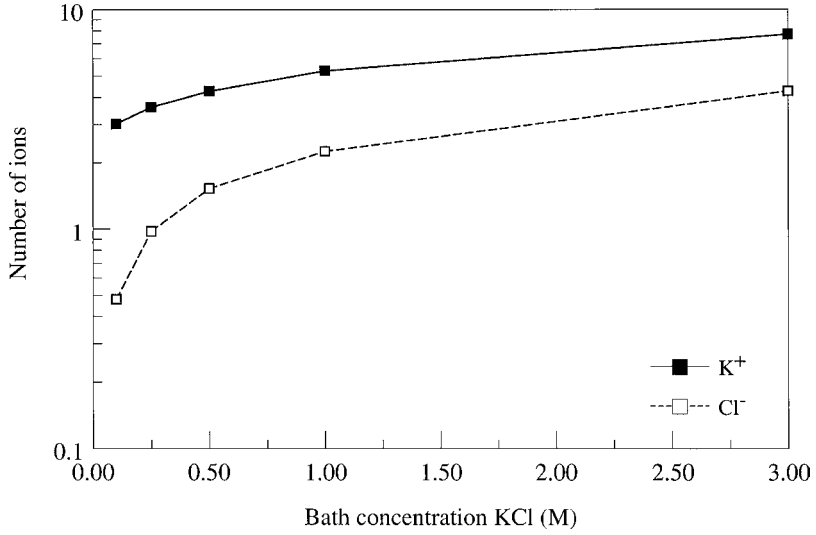

Figure 15. Net K^+ and Cl^- occupancy in the pore constriction ($z = 30$–40 Å) as a function of symmetric KCl bath concentration.

the channel, except at very high (3 M) salt concentration, presumably because of the electrostatic attraction of the K^+ to the negative charge residing on the channel. In contrast, the Cl^- occupancy inside the channel is always lower than in the bulk electrolyte.

This preference for cations over anions is even clearer in Figs. 14 and 15, which show respectively the total occupancy for a single pore, and the occupancy in the constriction region, for the same range of bath concentrations.

5. Conclusion

We have demonstrated that the continuum Poisson Drift-Diffusion model provides a useful tool for studying ion transport in open protein channel systems over time scales that cannot be resolved practically by detailed molecular dynamics or quantum approaches. Using ion diffusivity as the only adjustable parameter, we have computed the open channel current-voltage characteristics for a single *ompF* porin molecule, for a wide range of symmetric and asymmetric solutions

of KCl. At low salt concentrations the comparison between measured and computed I-V curves is reasonably good; the simulations reveal the rectifying properties of the channel that are also seen experimentally. At higher salt concentrations where the I-V characteristics are more linear the computed curves match the measured curves very well. In all cases, the calibrated K^+ and Cl^- ion diffusivities agree to within a factor of 3 with the experimentally determined values for bulk salt solution.

The usefulness of the continuum Poisson Drift-Diffusion formalism lies in its ability to reproduce the input-output characteristics of the system, using a fitted diffusivity. For a single isolated channel system, a spatially uniform diffusivity is adequate for such purposes. However, for multiple channel systems coupled together the ion diffusivity in the bath solutions connecting the channels must be unique. Given the recent evidence for two separate permeation pathways for cationic and anionic current (Im and Roux 2001, Schirmer and Phale 1999) it is unlikely that K^+ and Cl^- will have the same profile of diffusion coefficient, despite the fact that their values in bulk solution agree to within a few percent. Work is currently in progress to develop a position-dependent model for the ion diffusivity, inferred from the ion mean square deviation correlation function obtained from Molecular Dynamics simulations. The goal is to determine a diffusivity profile for each ionic species that returns to the correct bulk value in the baths and yields the measured channel I-V characteristics.

In addition, Poisson Drift-Diffusion theory, as it is presented here, does not include any representation of the finite ion volume, treating the ions as though they occupy a negligible fraction of the total volume of the system. The use of a continuum model to describe ion flow in regions where the ion diameter is comparable with the pore dimensions requires special care however, since the ion volume and the charge distribution introduce entropic and electrostatic effects that are not accounted for in the present formalism. Extension of the drift-diffusion model to include the effect of the finite ion size by introducing a correction to the total electrochemical potential of the system is the subject of ongoing work.

Acknowledgments

The authors are grateful Professor Tilman Schirmer and Dr. Raimund Dutzler for providing the molecular structure of *ompF* and for valuable discussions; to Dr. Duanpin Chen, Professor Eric Jakobsson, Dr. See-Wing Chiu and Sameer Varma for helpful discussions; to Professor Bob Dutton, Dr. Zhiping Yu and Dr. Dan Yergeau for assistance with PROPHET implementations. This work was supported by financial grants from the National Science Foundation (KDI Grant No. 9873199), Defense Advanced Research Projects Agency (DARPA F30 602-012-0513) and by the National Center for Supercomputing Applications (NCSA).

References

Alder B.J. 1992. In M. Mareschal and B. L. Holian (Ed.), Microscopic Simulations of Complex Hydrodynamic Phenomena. Plenum Press, New York, p. 425–430.

Antosiewicz J., Gilson M.K., Lee I.H., and McCammon J.A., 1995. Acetylcholinesterase: Diffusional encounter rate constants for dumbbell models of ligand. Biophysical Journal 68: 62.

Antosiewicz J., McCammon J.A., and Gilson M.K. 1994. Prediction of pH-dependent properties of proteins. Journal of Molecular Biology 238: 415.

Ashcroft F.M. 1999. Ion Channels and Disease. Academic Press, New York, p. 481.

Bagchi B. and Biswas R. 1998. Ionic mobility and ultrafast solvation: Control of a slow phenomenon by fast dynamic. Accounts of Chemical Research 31: 181.

Bank R.E., Burgler J., Coughran W.M., Jr., Fichtner W., and Smith R.K. 1990. Recent progress in algorithms for semiconductor device simulation. International Series on Numerical Mathematics 93: 125.

Bank R.E., Rose D.J., and Fichtner W. 1983. Numerical methods for semiconductor device simulation. IEEE Transactions on Electron Devices ED-30(9): 1031.

Barcilon V. 1992. Ion flow through narrow membrane channels: Part I. SIAM Journal on Applied Mathematics 52: 1391.

Barcilon V., Chen D., Eisenberg R.S., and Ratner M. 1993. Barrier crossing with concentration boundary conditions in biological channels and chemical reactions. Journal of Chemical Physics 98: 1193.

Barcilon V., Chen D.P., and Eisenberg R.S. 1992. Ion flow through narrow membranes channels: Part II. SIAM Journal on Applied Mathematics 52: 1405.

Barcilon V., Cole J., and Eisenberg R.S. 1971. A singular perturbation analysis of induced electric fields in nerve cells. SIAM Journal on Applied Mathematics 21(2): 339.

Barthel J., Buchner R., and Münsterer M. 1995. Electrolyte Data Collection Vol. 12, Part 2: Dielectric Properties of Water and Aqueous Electrolyte Solutions. DECHEMA, Frankfurt am Main.

Barthel J., Krienke H., and Kunz W. 1998. Physical Chemistry of Electrolyte Solutions: Modern Aspects. Springer, New York.

Berry S.R., Rice S.A., and Ross J. 2000. Physical Chemistry. Oxford University Press, New York, Oxford, p. 1064.

Cardenas A.E., Coalson R.D., and Kurnikova M.G. 2000. Three-dimensional Poisson-Nernst-Planck studies: Influence of membrane electrostatics on gramicidin a channel conductance. Biophysical Journal 79: 80.

Chen D., Eisenberg R., Jerome J., and Shu C. 1995. Hydrodynamic model of temperature change in open ionic channels. Biophysical Journal 69: 2304.

Chen D.P. and Eisenberg R.S. 1993. Charges, currents and potentials in ionic channels of one conformation. Biophysical Journal. 64: 1405.

Ciccotti G. and Hoover W.G. (eds.). 1990. Molecular-Dynamics Simulations of Statistical-Mechanical Systems. North Holland, New York, p. 326.

Conway B.E. 1969. Electrochemical Data. Greenwood Press Publishers, Westport CT, p. 374.

Conway B.E., Bockris J.O.M., and Yaeger E. (eds.). 1983. Comprehensive Treatise of Electrochemistry. Plenum, New York, p. 472.

Cowan S.W., Schirmer T., Rummel G., Steiert M., Ghosh R., Pauptit R.A., Jansonius J.N., and Rosenbusch J.P. 1992. Crystal structures explain functional properties of two *E. coli* porins. Nature 358: 727.

Davis H.T. 1996. Statistical Mechanics of Phases, Interfaces, and Thin Films. Wiley-VCH, New York, p. 712.

Durand-Vidal S., Simonin J.-P., and Turq P. 2000. Electrolytes at Interfaces. Kluwer, Boston.

Eisenberg R.S. 1986. Impedance measurements as estimators of the properties of the extracellular space. Annals of the New York Academy of Science 481: 116.

Eisenberg R.S. 1996. Computing the field in proteins and channels. Journal of Membrane Biology 150: 1.

Eisenberg R.S. 1999. From structure to function in open ionic channels. Journal of Membrane Biology 171: 1.

Eisenberg R.S. and Mathias R.T. 1980. Structural analysis of electrical properties of cells and tissues. CRC Critical Reviews in Bioengineering 4(3): 203.

Eisenberg R.S., Barcilon V., and Mathias R.T. 1979. Electrical properties of spherical syncytia. Biophysical Journal 25(1): 151.

Eisenberg R.S., Klosek M.M., and Schuss Z. 1995. Diffusion as a chemical reaction: Stochastic trajectories between fixed concentrations. Journal of Chemical Physics 102: 1767.

Evans D.J. and Morriss G.P. 1990. Statistical Mechanics of Nonequilibrium Liquids. Academic Press, New York, p. 302.

Ferry D.K. 1991. Semiconductors. McMillan Publishing Company, New York.

Gillespie D. and Eisenberg R.S. 2002. Physical descriptions of experimental selectivity measurements in ion channels. European Biophysics Journal 31: 454.

Harned H.S. and Owen B.B. 1958. The Physical Chemistry of Electrolytic Solutions. Reinhold Publishing Corporation, New York.

Hess K. 2000. Advanced Theory of Semiconductor Devices. IEEE Press, New York, p. 350.

Hille B. 2001. Ionic Channels of Excitable Membranes. Sinauer Associates Inc., Sunderland, p. 388.

Hodgkin A.L. 1937. Evidence for electrical transmission in nerve. I. Journal of Physiology 90: 183.

Hodgkin A.L. 1992. Chance and Design. Cambridge University Press, New York, p. 401.

Hollerbach U., Chen D., Nonner W., and Eisenberg B. 1999. Three-dimensional Poisson-Nernst-Planck theory of open channels. Biophysical Journal 76: A205.

Honig B. and Nichols A. 1995. Classical electrostatics in biology and chemistry. Science 268: 1144.

Hoover W. 1986. Molecular Dynamics. Springer-Verlag, New York, p. 138.

Hoover W.G. 1991. Computational Statistical Mechanics. Elsevier, New York, p. 313.

http://hoshi-o.physiology.uiowa.edu/Mutations/Home.html

Im W. and Roux B. 2001. Brownian dynamics simulations of ions channels: A general treatment of electrostatic reaction fields for molecular pores of arbitrary geometry. Biophysical Journal 115(10): 4850.

ISE Integrated System Engineering TCAD software (http://www.ise.ch).

Jack J.J.B., Noble D., and Tsien R.W. 1975. Electric Current Flow in Excitable Cells. Clarendon Press, New York, Oxford.

Jorgensen W.L. 1998. OPLS force fields. In P.v.R. Schleyer (Ed.), The Encyclopedia of Computational Chemistry, John Wiley & Sons Ltd., Athens, USA.

Jorgensen W.L. and Tirado-Rives J. 1988. The OPLS (Optimized Potentials for Liquid Simulations) potential functions for proteins, energy minimizations for crystals of cyclic peptides and crambin. Journal of the American Chemical Society 110: 1657.

Kurnikova M.G., Coalson R.D., Graf P., and Nitzan A. 1999. A lattice relaxation algorithm for 3-D Poisson-Nernst-Planck theory with application to ion transport through the gramicidin a channel. Biophysical Journal 76: 642.

Kurnikova M.G., Waldeck D.H., and Coalson R.D. 1996. A molecular dynamics study of the dielectric friction. Journal of Chemical Physics 105(2), 628.

Lide D.R. 1994. (editor-in-chief), CRC Handbook of Chemistry and Physics. CRC press, Boca Raton, p. 5–90.

Lundstrom M. 1992. Fundamentals of Carrier Transport. Addison-Wesley, New York.

Mareschal M. and Holian B.L. (eds.). 1992. Microscopic Simulations of Complex Hydrodynamic Phenomena. Plenum Press, New York.

Mathias R.T., Levis R.A., and Eisenberg R.S. 1980. Electrical models of excitation-contraction coupling and charge movement in skeletal muscle. Journal of General Physiology 76(1): 1.

Mauro A., Blake M., and Labarca P. 1988. Voltage gating of conductance in lipid bilayers induced by porin from outer membrane of Neisseria Gonorrhoease. Proceedings of the National Academy of Science 85: 1071.

Nee T.-w. and Zwanzig R. 1970. Theory of dielectric relaxation in polar liquids. Journal of Chemical Physics 52: 6353.

Newman J.S. 1991. Electrochemical Systems. Prentice-Hall, Englewood Cliffs, NJ, p. 560.

Nonner W., Catacuzzeno L., and Eisenberg B. 2000. Binding and selectivity in L-type Ca channels: A mean spherical approximation. Biophysical Journal 79: 1976.

Nonner W., Gillespie D., and Eisenberg B. 2002. Flux and selectivity in the Ca channel: A density functional approach. Biophysical Journal 82: 340a.

Nonner W., Gillespie D., Henderson D., and Eisenberg B. 2001. Ion accumulation in a biological calcium channel: Effects of solvent and confining pressure. Journal of Physical Chemistry B 105: 6427.

Phale P.S., Philippsen A., Widmer C., Phale V.P., Rosenbusch J.P., and Schirmer T. 2001. Role of charged residues at the OmpF porin channel constriction probed by mutatgenesis and simulation. Biochemistry 40: 6319.

Philippsen A., Im W., Engel A., Schirmer T., Roux B., and Muller D.J. 2002. Imaging the electrostatic potential of transmembrane

channels: Atomic probe microscopy of Ompf porin. Biophysical Journal 82(3): 1667.

PROPHET Web site at Stanford University (http://www-tcad.stanford.edu/~prophet/).

Ravaioli U. 1998. Hierarchy of simulation approaches for hot carrier transport in deep submicron devices. Semiconductor Science and Technology 3: 1–10.

Robinson R.A. and Stokes R.H. 1959. Electrolyte Solution. Butterworths Scientific Publications, London.

Roux B. 1999. Statistical mechanical equilibrium theory of selective ion channels. Biophysical Journal 77: 139.

Roux B. and Karplus M. 1991. Ion transport in a gramicidin-like channel: Dynamics and mobility. Journal of Physical Chemistry 95: 4856.

Roux B. and Karplus M. 1991. Ion transport in a model gramicidin channel. Structure and thermodynamics. Biophysical Journal 59: 961.

Saint N., Lou K.-L., Widmer C., Luckey M., Schirmer T., and Rosenbusch J.P. 1996. Structural and functional characterization of Ompf porin mutants selected for large pore size. II. Functional characterization. Journal of Biological Chemistry 271(34): 20676.

Saint N., Prilipov A., Hardmeyer A., Lou K.-L., Schirmer T., and Rosenbusch J. 1996. Replacement of the Sole Hisdinyl Residue in Ompf Porin from *E. coli* by threonine (H21t) does not affect channel structure and function. Biochemical and Biophysical Research Communications 223: 118.

Schindler H. and Rosenbusch J.P. 1978. Matrix protein from *Escherichia coli* outer membranes form voltage controlled channels in lipid bilayers. Proceedings of the National Academy of Science USA 75: 3751.

Schirmer T. 1998. General and specific porins from bacterial outer membranes. Journal of Structural Biology 121: 101.

Schirmer T. and Phale P.S. 1999. Brownian dynamics simulation of ion flow through porin channels. Journal of Molecular Biology 294: 1159.

Schmickler W. 1996. Interfacial Electrochemistry. Oxford University Press, New York.

Schuss Z., Nadler B., and Eisenberg R.S. 2001. Derivation of Poisson and Nernst-Planck equations in a bath and channel from a molecular model. Physical Review E 64: 036116-1.

Selberherr S. 1984. Analysis and Simulation of Semiconductor Devices. Springer-Verlag, Vienna.

Sharp K. and Honig B. 1990. Electrostatic interactions in macromolecules: Theory and applications. Annual Review of Biophysics and Bioengineering 19:301.

Shockley W. 1950. Electrons and holes in semiconductors. Van Nostrand, Princeton, NJ.

Silvaco TCAD (http://www.silvaco.com).

Simonin J.-P. 1997. Real ionic solutions in the mean spherical approximation. 2. Pure strong electrolytes up to very high concentrations and mixtures, in the primitive model. Journal of Physical Chemistry B 101: 4313.

Simonin J.-P. and Blum L. 1996. Departures from ideality in pure ionic solutions using the mean spherical approximation. Journal of the Chemical Society, Faraday Transactions 92: 1533.

Simonin J.-P., Bernard O., and Blum L. 1998. Real ionic solutions in the mean spherical approximation. 3. Osmotic and activity coefficients for associating electrolytes in the primitive model. Journal of Physical Chemistry B 102: 4411.

Simonin J.-P., Bernard O., and Blum L. 1999. Ionic solutions in the binding mean spherical approximation: Thermodynamic properties of mixtures of associating electrolytes. Journal of Physical Chemistry B 103: 699.

Simonin J.-P., Blum L., and Turq P. 1996. Real ionic solutions in the mean spherical approximation. 1. Simple salts in the primitive model. Journal of Physical Chemistry 100: 7704.

Synopsis TCAD (http://www.synopsys.com).

Tieleman D.P. and Berendsen H.J.C. 1998. A molecular dynamics study of the pores formed by *Escherichia Coli* Ompf Porin in a fully hydrated palmitoyloleoylphosphatidylcholine bilayer. Biophysical Journal 74: 2786.

Tieleman D.P., Biggin P.C., Smith G.R., and Sansom M.S.P. 2001. Simulation approaches to ion channel structure-function relationships. Quarterly Reviews of Biophysics 34: 473.

Tyrrell H.J.V. and Harris K.R. 1984. Diffusion in Liquids. Butterworths Monographs in Chemistry, Boston.

Valdiosera R., Clausen C., and Eisenberg R.S. 1974. Circuit models of the passive electrical properties of frog skeletal muscle fibers. Journal of General Physiology 63: 432.

van der Straaten T., Varma S., Chiu S.-W., Tang J., Aluru N., Eisenberg R., Ravaioli U., and Jakobsson E. 2002. Combining computational chemistry and computational electronics to understand protein ion channels. In The Technical Proceedings of the Second International Conference on Computational Nanoscience and Nanotechnology, pp. 60–63.

Waisman E. and Lebowitz J.L. 1972. Mean spherical model integral equation for charged hard spheres. I. Method of solution. Journal of Chemical Physics 56: 3086.

Waisman E. and Lebowitz J.L. 1972. Mean spherical model integral equation for charged hard spheres. II. Spheres. Journal of Chemical Physics 56: 3093.

Warshel A. and Russell S.T. 1984. Calculations of electrostatic interactions in biological systems and in solutions. Quarterly Review of Biophysics 17: 283.

Weiss M.S. and Schulz G.E. 1992. Structure of porin refined at 1.8 Å resolution. Journal of Molecular Biology 227: 493.

Wolynes P. 1980. Dynamics of electrolyte solutions. Annual Reviews Physical Chemistry 31: 345.

Young J.D., Blake M., Mauro A., and Cohn Z.A. 1983. Properties of the major outer membrane protein from Neisseria Gonorrhoeae incorporated into model lipid membranes. Proceedings of the National Academy of Science 80: 3831.

Zematis Jr., J.F., Clark D.M., Rafal M., and Scrivner N.C. 1986. Handbook of Aqueous Electrolyte Thermodynamics. Design Institute for Physical Property Data, American Institute of Chemical Engineers, New York.